The Condensin Complex Governs Chromosome Condensation and Mitotic Transmission of rDNA

Lita Freeman, Luis Aragon-Alcaide, and Alexander Strunnikov

Unit of Chromosome Structure and Function, National Institutes of Health, National Institute of Child Health and Human Development, Laboratory of Molecular Embryology, Bethesda, Maryland 20892-5430

Abstract. We have characterized five genes encoding condensin components in *Saccharomyces cerevisiae.* All genes are essential for cell viability and encode proteins that form a complex in vivo. We characterized new mutant alleles of the genes encoding the core subunits of this complex, *smc2-8* and *smc4-1*. Both *SMC2* and *SMC4* are essential for chromosome transmission in anaphase. Mutations in these genes cause defects in establishing condensation of unique (chromosome VIII arm) and repetitive (rDNA) regions of the genome but do not impair sister chromatid cohesion. In vivo localization of Smc4p fused to green fluorescent protein showed that, unexpectedly, in *S. cerevisiae* the condensin complex concentrates in the rDNA region at the G2/M phase of the cell cycle. rDNA segregation in mitosis is delayed and/or stalled in *smc2* and *smc4* mutants, compared with separation of pericentromeric and distal arm regions. Mitotic transmission of chromosome III carrying the rDNA translocation is impaired in *smc2* and *smc4* mutants. Thus, the condensin complex in *S. cerevisiae* has a specialized function in mitotic segregation of the rDNA locus. Chromatin immunoprecipitation (ChIP) analysis revealed that condensin is physically associated with rDNA in vivo. Thus, the rDNA array is the first identified set of DNA sequences specifically bound by condensin in vivo. The biological role of higher-order chromosome structure in *S. cerevisiae* is discussed.

Key words: SMC • condensin • chromosome condensation • chromosome segregation • chromatin

Introduction

The relationship between higher-order structure and function in the eukaryotic chromosome is not well-understood. Chromosomes are functionally complex, supporting DNA replication, transcription, silencing, DNA repair, genetic recombination, and mitotic segregation. The long-range architecture of the chromosomes must accommodate, and in some cases, even determine these disparate chromosomal functions. Identifying molecules involved in long-range chromosome organization and determining their functional roles is crucial to understanding chromosome architecture.

Recent work has identified a family of proteins determining proper chromosome structure in the mitotic cell cycle, the SMC proteins (Koshland and Strunnikov, 1996; Strunnikov, 1998; Hirano, 1999). The predicted structure of SMC proteins includes an NH_2-terminal nucleoside triphosphate binding site, two long helical-coil regions separated by a hinge, and a COOH-terminal DA box. These features have become signature motifs for the SMC family. The first SMC protein characterized in *Saccharomyces cerevisiae,* Smc1p, was identified upon analysis of *smc1* mutants in *S. cerevisiae* (Strunnikov et al., 1993). The *S. cerevisiae* genome sequencing project revealed the presence of three more *SMC* family genes, *SMC2*, *SMC3*, and *SMC4* (Koshland and Strunnikov, 1996). The *SMC1* and *SMC3* genes are involved in sister chromatid cohesion (Michaelis et al., 1997), whereas the *smc2* mutants show defects in long-range structure, i.e., maintenance of condensation (Strunnikov et al., 1995). The *Schizosaccharomyces pombe SMC2* and *SMC4* orthologues, cut14 and cut3, respectively, and associated factors, are required for mitotic chromosome condensation and segregation (Saka et al., 1994; Sutani et al., 1999), perhaps by using an ATP-independent DNA binding and reannealing activity (Sutani and Yanagida, 1997). The *Bacillus subtilis* SMC homodimer, important for proper bacterial chromosome partitioning (Britton et al., 1998; Graumann et al., 1998), reanneals ssDNA in vitro (Hirano and Hirano, 1998).

Studies in higher eukaryotes fully concur with *S. cerevisiae* and *S. pombe* data, implicating roles for Smc2 and

Address correspondence to Alexander Strunnikov, Laboratory of Molecular Embryology, National Institutes of Health, National Institute of Child Health and Human Development, Unit of Chromosome Structure and Function, 18T Library Drive, Room 106, Bethesda, MD 20892-5340. Tel.: (301) 402-1323. Fax: (301) 402-1323. E-mail: strunnik@box-s.nih.gov

Smc4 proteins in mitotic chromosome structure. The chicken orthologue of Smc2p, ScII, localizes to mitotic chromosomes (Saitoh et al., 1994). Two *Xenopus laevis* proteins orthologous to Smc2p and Smc4p, termed XCAP-E and XCAP-C, respectively, copurify with in vitro–assembled mitotic chromosomes and localize to mitotic chromosomes in vivo (Hirano and Mitchison, 1994). XCAP-C and XCAP-E form a 13S condensin complex required for mitotic chromosome condensation in vitro (Hirano et al., 1997), along with XCAP-H, XCAP-D2, and XCAP-G. XCAP-H is the homologue of the *Drosophila melanogaster* Barren protein, mutations in which cause mitotic defects in embryos with formation of chromosome bridges (Bhat et al., 1996). XCAP-D2 is almost identical to pEg7, which concentrates on chromosomes during mitosis and which is important for condensation and resolution of mitotic chromosomes (Cubizolles et al., 1998). The 13S–condensin complex induces ATP-dependent positive supercoiling of a DNA template as a result of its stoichiometric binding to DNA (Kimura and Hirano, 1997; Kimura et al., 1999). This supercoiling activity depends on phosphorylation, probably by the CDC2 kinase (Kimura et al., 1998).

In addition to the role in mitotic chromosome condensation, some condensin subunits can have additional roles in chromosome structure and function. In *Caenorhabditus elegans*, a specialized homologue of Smc4p, DPY-27, is a part of a dosage compensation complex (Chuang et al., 1994, 1996). Another *C. elegans* protein MIX-1, an orthologue of Smc2p, is involved in both mitosis and dosage compensation (Lieb et al., 1998).

In *S. cerevisiae*, chromosome condensation occurs on a fairly minor scale (Guacci et al., 1994). Thus, it was not known whether the condensin complex exists in budding yeast, what the biological role of condensation in *S. cerevisiae* is, or why condensation of the relatively short *S. cerevisiae* chromosomes is required. Also unknown is the mechanism by which *smc2* mutations block full separation of chromatids in anaphase (Strunnikov et al., 1995). To disentangle these unresolved issues, we have initiated a systematic analysis of all factors required for chromosome condensation in a genetically and biochemically tractable organism, *S. cerevisiae*. We investigate the genes encoding condensin subunits, with an emphasis on the core condensin components, Smc2p and Smc4p, with respect to their roles in chromosome transmission in anaphase and in chromosome condensation in vivo.

Materials and Methods

Cloning and DNA Sequencing

Cloning of the *SMC2* gene has been reported previously (Strunnikov et al., 1993, 1995). Sequence information for the *SMC4*, *BRN1*, *YCS4*, and *YCS5* genes was obtained from the Yeast Genome Project (Galibert et al., 1996; Johnston et al., 1997). The *SMC4* gene containing flanking EcoRI and SphI sites was assembled from two genomic PCR products (S288c background). The resulting fragment was cloned into YCplac111 giving pAS534. The BamHI-SphI fragment of pAS534 was cloned into YCplac33 (Gietz and Sugino, 1988) giving pAS546. The wild-type *SMC4* gene was also isolated as a plasmid (pAS574) complementing the *smc4-1* mutation (library reference in Guacci et al., 1997). DNA was sequenced using the ABI Prism 377 dye-terminator method (PerkinElmer). Sequence analysis was performed using AssemblyLign software (Oxford Molecular).

Strains, Plasmids and Genetic Techniques

Yeast strains used are shown in Table I. In all listed cases of plasmid integration, the confirmation was obtained by Southern blotting, PCR, or Western blotting. The *smc4–Δ1::HIS3* and *smc4–Δ2::URA3* deletions were constructed by transforming AS260 (Strunnikov et al., 1995) with fragments from plasmids pAS518 or pAS531, respectively. Haploid deletion strains were isolated as meiotic progeny of heterozygous diploid strains and were maintained with a minichromosome containing the corresponding wild-type *SMC* gene. Disruption of the *SMC2* gene was according to Strunnikov et al. (1995). The *brn1–Δ::URA3* disruption allele was constructed using primers designed to amplify markers from the pRS416 vector (TGAAAATAACGATGACGATGAAAGAGTAGAATATAATCTCTTTACCAATAGAGATTGTACTGAGAGTGCACC/GTCATTATAGTTTTCGGTATGAGTTATCTGCAACCCATGCTCATTGGCTAAGTGTGCGGTATTTCACACCGC). The corresponding PCR product was directly used to transform AS400 and AS401. The *ycs4* and *ycs5* deletion alleles were constructed using the same strategy with the primer pairs TTACTGTTGTAAAAAGAAAGACTAATGGCC TTTGTCAATTGCACTTTGGGTAAATTGTACTGAGAGTGCACC/TGGGTCTCGCACTTTCTCAGTCTTCCAACTAATTTCTCGTTTAATTGCTTTTGGTGCGGTATTTCACACCGC and GAGTTATTGCGACTTTTAAAATCCGTGCACCGCATATGAAAGGGTAGAGCCTTCGTGTACTGAGAGTGCACC/TGTCCCACCGGGTAATGTGCGTAATGCAATAACATATAGCATCTATATCTGGTAAGCGGTATTTCACACCGC, respectively. The resulting diploids were analyzed by tetrad dissection.

SMC2 mutagenesis by PCR was as described previously (Strunnikov et al., 1995). The *smc2-8* allele was integrated into the chromosome as described previously for *smc2-6* (Strunnikov et al., 1995). To generate temperature-sensitive mutants of *SMC4*, pAS534 was transformed into the XL-Red strain (Stratagene). Plasmid DNA was isolated and transformed into strain 16aAS335/pAS546. Plasmid shuffling resulted in isolation of pAS534/1 containing the *smc4-1* temperature-sensitive allele. The *smc4-1* allele was introduced into the chromosome via *smc4–Δ2::URA3* allele replacement.

The green fluorescent protein (GFP)[1]-based chromosome tagging system for yeast chromosome V was designed by modification of the pAFS135 and pAFS59 vectors (Straight et al., 1996). Plasmid pAFS135 expressing LacI-GFP was digested with NsiI, and the PstI-NsiI fragment of the *URA3* gene was inserted to create pAS545. This plasmid was targeted to the *ura3* locus by digestion of pAS545 with StuI. Tandem *LacO* repeats were subsequently introduced into the same locus by integrating pAS399 digested with ScaI into pAS545. pAS399 was created by ligating the BamHI-SalI fragment of pAFS59 into the BamHI and XhoI sites of pRS404. The resulting strains were maintained in media lacking histidine and tryptophan to prevent loss of integrated constructs due to mitotic recombination. For chromosome IV arm probe tandem *LacO* repeats were introduced into *ADE8* locus by integrating pLA754 digested with Asp718-I. pLA754 was created by insertion of truncated *ADE8* gene into XhoI and SacI sites of pAFS59. The resulting strains containing pAS545 and pLA754 were maintained in media lacking histidine and leucine.

Smc4p was tagged by fusing GFP by PCR to the 3′ end of the gene, creating pLF640 (3′ *SMC4-GFP*). This plasmid was targeted into the chromosomal *SMC4* locus by AgeI digestion, disrupting the untagged gene. The Smc4p-GFP fusion was fully functional in vivo.

To tag *SMC2* with the hemagglutinin (HA) epitope, haploid strain YPH499bp was transformed with a XbaI-SalI fragment from plasmid pAS532, replacing the untagged gene. This fragment carries the *SMC2* gene with a PCR-generated 12His-3HA tag inserted into its SpeI site and an upstream *LEU2* marker. To epitope-tag *YCS5*, two primers, ATGTCCATAGATGAAGAAGATAAGGATTCAGAGTCTTTCAGCGAGGTCTGTCTAGTTGGTGGCGGCCACCAC and AGCGTAGAAGAATTAACAAACCTAAGAATAAAATACAAATATGTTTACAAGAGATTCCCGGGTAATAACTGA, were used to amplify a fragment of pAS660 (Strunnikov, A., unpublished data) containing the 12His-3HA tag immediately followed by the *URA3* gene. The resulting PCR product containing the arms homologous to the 3′ end of *YCS5* was transformed directly into YPH499bp giving YPH499bp5. *BRN1* and *YCS4* were tagged using the same strategy with the following pairs of primers, respectively: ATGACTTGATAGTGAATTATGAGGATCTAGCGA-

[1]*Abbreviations used in this paper:* ARS, DNA replication origin; ChIP, chromatin immunoprecipitation; FISH, fluorescent in situ hybridization; GFP, green fluorescent protein; HA, hemagglutinin; YAC, yeast artificial chromosome.

Table I. S. cerevisiae Strains

Strain	Relevant genotype
AS400	*MATa/MATα LEU2/leu2 MET15/met15 TRP1/trp1 ura3*
YPH499bp	*MATa ura3 lys2 ade2 trp1 his3 leu2 bar1-Δ, pep4::HIS3*
YPH499bp2	*YPH499bp, SMC2:12His:3HA(LEU2)*
YPH499bp5	*YPH499bp, YCS5:12His:3HA(URA3)*
YPH499bp6	*YPH499bp, BRN1:12His:3HA(URA3)*
BY4733bp4	*MATa his3 leu2 met15 trp1 ura3 YCS4:12His:3HA(URA3) bar1-Δ::LEU2 pep4::HIS3*
16aAS335/pAS546	*MATa ade2 his3 leu2 lys2 ura3 smc4-Δ1::HIS3 / URA3 SMC4*
1bAS330	*MATa smc2-8 ade2 leu2 lys2 his3 trp1 ura3*
1bAS344	*MATa smc4-1 ade2 his3 leu2 lys2 ura3*
3-1bAS330b/pAS622	*MATa ade2 leu2 lys2 his3 trp1 smc2-8 ura3 bar1Δ SIR2:GFP12(HIS3) SIR4-42::URA3*
6-1bAS344b/pAS622	*MATa ade2 his3 leu2 lys2 ura3 smc4-1 bar1Δ SIR2:GFP12(HIS3) SIR4-42::URA3*
YPH499bV	*MATa lys2 ade2 trp1 his3 bar1 ura3::(HIS3 lacl-GFP)::(TRP1 lacO)*
1bAS330bV	*MATa smc2-8 ura3::(HIS3 lacI-GFP)::(TRP1 lacO)*
1aAS342bV	*MATa smc4-1 ura3::(HIS3 lacI-GFP)::TRP1 lacO)*
1bAS330bIV	*MATa smc2-8 ura3::(HIS3 lacI-GFP) ade8::(LEU2 lacO)*
1aAS342bIV	*MATa smc4-1 ura3::(HIS3 lacI-GFP) ade8::(LEU2 lacO)*
AS335	*MATa/α ade2 his3 leu2 lys2 ura3 trp1/TRP1 smc4-Δ1::HIS3*
NOY891/pNOY353	*MATa ade2 ura3 leu2 his3 can1 rdn1-ΔΔ::HIS3 / TRP1 pGAL7:rDNA* (Oakes et al., 1998)
AS401	*MATa/MATα ade2 ura3 leu2 his3 can1 rdn1-ΔΔ::HIS3 / TRP1 pGAL7:rDNA*
L4078	*MATa ade2 leu2 lys2 trp1 ura3 his5 III::(LEU2::ADE2::rDNA::URA3)* (G. Fink)
AS389	*MATa/MATα ade2 leu2 lys2 ura3 leu2 TRP1/trp1 III/III::(LEU2::ADE2::rDNA::URA3)*
AS388	*MATa/MATα ade2 leu2 lys2 ura3 TRP1/trp1 smc2-8 III/III::(LEU2::ADE2::rDNA::URA3)*
AS386	*MATa/MATα ade2 leu2 lys2 ura3 smc4-1 III/III::(LEU2::ADE2::rDNA::URA3)*
4419	*MATa ade2-1 lys2-1 can1-100 trp1 ura3 his5 / ADE2 HIS3* (200 kb)
6228	*MATa ade2-1 lys2-1 can1-100 trp1 ura3 his5 / ADE2 HIS3* (900 kb)
2aAS415	*MATa smc2-8 ade2 his3 / ADE2 HIS3* (200 kb)
1aAS416	*MATa smc4-1 ade2 his3 / ADE2 HIS3* (200 kb)
5bAS413	*MATa smc2-8 ade2 his3 / ADE2 HIS3* (900 kb)
1aAS414	*MATa smc4-1 ade2 his3 / ADE2 HIS3* (900 kb)
AS260-1	*MATa/MATα ade2 his3 leu2-Δ1/leu2-Δ::ADE2 lys2 trp1/TRP1 ura3*
AS359-1	*MATa/MATα ade2 leu2/leu2-Δ::ADE2 lys2 his3 TRP1/trp1 ura3 smc2-8*
AS362-1	*MATa/α ade2 his3 leu2-Δ1/leu2-Δ::ADE2 lys2 ura3-52 smc4-1*
WY53	*MATa ade2 his3 leu2 trp1 ura3 net1::9Myc-NET1::LEU2 pep4-Δ* (Shou et al., 1999)

CAACACAGGCAGCGTCACTAGTTGGTGGCGGCCACCACC/ATCCACTTTTCGAAGCGGTCCCCTTTCGGCGATAAAGGATTTCGTAAGCCGAGATTCCCGGGTAATAACTGA and GACGTCACTGCATTATTGGAGCAAGGTTTCAAGGTTGTATCCGCAAAAGAACTAGTTGGTGGCGGCCACCAC/ATTTTATCGAGATAGGTAAAGTCATATTTCAAGAAGAAAGAAATGAACAGGAGATTCCCGGGTAATAACTGA.

To generate chromosome III labeled with *ADE2*, the *leu2* allele was replaced in a one-step transformation by the PCR product generated from the wild-type *ADE2* gene using primers TGGTCAAGAAATCACAGCCGAAGCCATTAAGGTTCTTAAAGCTATTTCTGATGTTCGTGAATAATACATAAC and TTGCTTACCTGTATTCCTTTACTATCCTCCTTTTTCTCCTTCTTGATAAATGTATGAAATTCTTAAAAAAAGG. The mutant strains with the rDNA translocations were generated by genetic crosses to L4078.

Cell Cycle Methods

Yeast cultures were maintained according to standard techniques (Rose et al., 1990). Yeast cell cycle experiments were conducted as described previously (Strunnikov et al., 1995; Guacci et al., 1997) with minor modifications. To double-block with α-factor and nocadazole for GFP-mediated visualization of sister chromatid separation, cells were first grown at 23°C in synthetic drop-out media lacking tryptophan and histidine to 5×10^6 cells/ml. α-Factor was then added to 10^{-8} M and cells were incubated 3 h at 23°C until 100% arrest in G1. Cells were washed three times with incubation media and incubated for 2 h at 37°C in the presence of 0.1 mg/ml pronase and 30 μg/ml nocadazole. The quality of arrest at all stages was monitored microscopically and by FACS®.

Antibodies and Immunoprecipitations

Anti-Smc2p, Smc4p, Brn1p, and Ycs4p antibodies were generated against the antigens expressed in the BL21(DE3)pLysS strain of *Escherichia coli* (Novagen). The expression plasmids contained the fragments encoding the last 590, 675, 418, and the first 390 amino acid residues of Smc2p, Smc4p, Brn1p, and Ycs4p, respectively. A XhoI *SMC2* fragment from pAS434 was ligated into XhoI-digested pRSETa, creating pLF555. A SalI-XhoI fragment from pAS515 containing the 3′ part of *SMC4* was ligated into XhoI-digested pRSETa, creating pLF554. A PCR-generated BamHI fragment of *BRN1* containing the 3′ end of the gene was ligated into BamHI-digested pRSETa, creating pAS636. A PCR-generated BamHI-BstBI fragment of *YCS4* containing the 3′ part of the gene was ligated into BamHI-BstBI–digested pRSETa, creating pLF656. The antigens were purified sequentially by immobilized metal affinity chromatography (ProBond; Invitrogen) and PAGE and then injected into two New Zealand white rabbits (Covance). Production sera were affinity purified on CNBr-Sepharose columns (Amersham Pharmacia Biotech) with the coupled purified recombinant protein and used for Western blotting. All commercially available antibodies were used according to manufacturer recommendations.

Immunoprecipitations were performed with EBX buffer (Liang and Stillman, 1997), except sonication and/or DNAse I (10 μg/ml, 15 min at 15°C) were used to fragment chromatin. All buffers contained Complete™ protease inhibitors (Boehringer). Lysates for immunoprecipitation reactions were prepared by the bead-beating method (Strunnikov et al., 1995). Cell lysates, diluted 1:10 in EBX, were incubated 6 h at 4°C with anti-HA antibodies (12CA5; Boehringer) coupled to CNBr-Sepharose beads. The beads were washed six times with 1 ml EBX in MicroBioSpin columns (BioRad). Proteins bound to antibodies were eluted in 200 μl 2% SDS at room temperature for 20 min, followed by 5 min incubation at 90°C.

Chromatin immunoprecipitation (ChIP) was performed exactly as in Meluh and Koshland (1997), with a cross-linking time of 1 h 15 min. For precipitation of Smc2p-HA–containing chromatin fragments, the polyclonal rabbit anti-HA antibody #2973 was generated by injecting a key-

hole limpet hemacyanin–coupled linear peptide corresponding to one and a half repeats of the HA tag (NH_3-GYPYDVPDYAG-COOH) into New Zealand white rabbits (Covance). Immunoprecipitated DNA was diluted at least 1:50 for PCR of rDNA compared with the unique region DNA ChIP.

Fluorescent In Situ Hybridization and Microscopy

Fluorescent in situ hybridization (FISH) was performed essentially as described (Guacci et al., 1994) with minor modifications in the cell-swelling protocol. rDNA probes were as in Guacci et al. (1997). Chromosome VIII FISH-painting probes prepared from cosmids C9315, C8179, C9666, C9925, C8025, C8082, and C9205 (ATCC) were labeled with digoxygenin separately as described (Guacci et al., 1994). Probes span a 230-kb region of chromosome VIII, including the centromere. All probes were titrated using a dot-blot filter assay for digoxygenin and then mixed for FISH experiments. The arrest protocol for the establishment of chromosome condensation included α-factor treatment at 23°C for 3 h with release into nocadazole-containing media at 37°C for 2 h. The cells were fixed in 4% formaldehyde for 2 h. The rDNA FISH signal was quantified using the Segmentation function of IP Lab (Scanalytics). The area of the FISH signal was divided by the area of the propidium iodide signal, thus giving the normalized measurement for each nucleus. In the case of multiprobe painting of chromosome VIII, minimal circles were drawn around the FISH signal and around the propidium iodide signal (see Fig. 3 C). The areas of the circles were then treated as segments in the rDNA quantitation.

Microscopy was performed using the wide-field Zeiss AxioVert microscope with epifluorescence. The images were collected using a MicroMax cooled charge-coupled device camera (Princeton Instruments) and Z-axis motor assembly (Ludl). Optical sections were converted into a stacked image with IP-Lab software (Scanalytics). For LacI-GFP chromosomal tag visualization, cells were fixed with 3.7% formaldehyde for 5 min, washed extensively with PBS, and mounted for microscopy in a minimal volume of PBS buffer. 10–20 optical sections spanning 5 μM were collected per each field. Distribution of GFP signal was quantified using the recorded three-dimensional images.

Results

Characterization of the Condensin Protein Complex in S. cerevisiae

The *SMC2* gene from *S. cerevisiae* has been characterized previously and found to be essential for viability and maintenance of chromosome condensation (Strunnikov et al., 1995). We disrupted the previously uncharacterized *S. cerevisiae SMC* gene *SMC4* (Koshland and Strunnikov, 1996) and three open reading frames encoding the putative condensin subunits *BRN1* (*XCAP-H* orthologue), *YLR272c* (*XCAP–D2* orthologue), and *YDR325w* (*XCAP–G* orthologue), revealed by the genome sequencing project. All genes were found to be essential for cell viability (see Materials and Methods). We designated the *YLR272c* gene *YCS4* and the *YDR325w* gene *YCS5*, for yeast condensin subunit four and five, respectively. Detailed sequence analysis of *SMC4*, *YCS4*, and *YCS5* (not shown) demonstrates that these proteins have conserved clusters of amino acid residues representing the characteristic signature motifs for each condensin subunit. Fig. 1 A shows classification of *S. cerevisiae* and some higher eu-

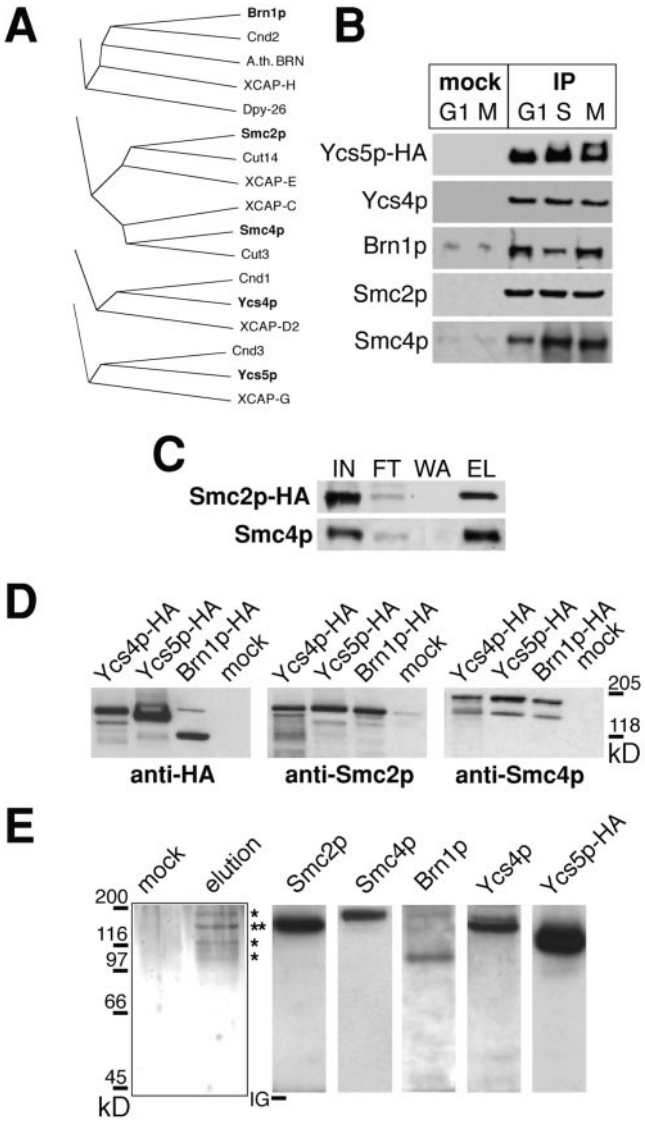

Figure 1. Characterization of the condensin protein complex. (A) CLUSTALW alignment of the condensin subunits from different organisms. *Arabidopsis thaliana* and human sequences are from GenBank. (B) Immunoprecipitation of condensin throughout the cell cycle. Strains YPH499bp (mock) and YP499bp5 were arrested with α-factor (G1, 100% of cells arrested), hydroxyurea (S, 84% arrest), and nocadazole (M, 96% arrest). 12CA5 immunoprecipitates from the corresponding protein extracts are shown for YPH499bp5. Smc2p, Smc4p, Brn1p, and Ycs4p are detected with the corresponding rabbit polyclonal antibodies. The precipitates were probed with antibodies against chromatin proteins, including Hmo1, Smc1p, Mcd1p, and Top2p, but no positive signal was detected (data not shown). (C) Smc2p and Smc4p form an obligatory complex. Asynchronous cells of YPH499bp2 were analyzed by immunoprecipitation. Saturating amount of anti-HA beads were added, allowing quantitative depletion of Smc2p-HA. IN, input; FT, flow-through; WA, wash; and EL, elution. (D) Stoichiometry of non-SMC condensin subunits. Extracts from YPH499bp6, BY4733bp4, and YPH499bp5, grown to equal optical density were analyzed by anti-HA immunoprecipitation. Immunoprecipitates were probed with anti-HA, anti-Smc2p, and anti-Smc4p antibodies. (E) Immunoaffinity purification of condensin complex. 10 g of the YPH499bp5 cell was subjected to the modified immunoprecipitation protocol, followed by the peptide elution with AS4 (GYPYDVPDYAG) (0.5 mg/ml) in place of SDS. 10 g of YPH499bp cells was processed identically for the mock purification. The silver-stained gel (4–12% PAGE) shows stoichiometry of condensin subunits. Asterisks indicate positions of the condensin subunit bands on the gel. Proteins were identified by Western blot with the corresponding antibodies. Smc2p (predicted molecular mass 134 kD) and Ycs4p (133 kD) comigrate.

karyotic condensin subunits into corresponding orthologous groups. Smc2p and Smc4p are the most conserved proteins in the complex and Ycs5p is the least evolutionary conserved.

To verify whether the putative condensin subunits indeed form a complex in *S. cerevisiae*, we generated epitope-tagged versions of the corresponding genes and raised antibodies against the putative condensin subunits (see Materials and Methods). Immunoprecipitation from extracts containing Ycs5p-HA using anti-HA antibody revealed that the precipitate contains other putative condensin subunits. Fig. 1 B shows that Ycs5p-HA immunoprecipitates contain Smc2p (predicted molecular mass 134 kD), Smc4p (162 kD), Brn1p (83 kD), and Ycs4p (133 kD) in addition to the tagged Ycs5p (126 kD). Only Brn1p showed abnormal PAGE mobility, migrating with an apparent molecular mass of 100 kD. Analysis of extracts from G1, S, and G2/M cells shows little dependence of complex composition on cell cycle stage (Fig. 1 B). Thus, a complex similar to the *X. laevis* 13S condensin is present in *S. cerevisiae*. We therefore called this five-subunit complex *S. cerevisiae* condensin. Analysis of whole cell extracts showed that Smc2p-HA is more abundant in the cell than Brn1p-HA, Ycs4p-HA, and Ycs5p-HA throughout the cell cycle (data not shown). This suggests that an incomplete condensin complex similar to the *X. laevis* 8S complex lacking non-SMC subunits may also exist in *S. cerevisiae*.

We analyzed the stoichiometry of condensin subunits in several experiments. As expected, complete immunoprecipitation of Smc2p-HA from extract led to complete depletion of Smc4p (Fig. 1 C). When immunoprecipitates of the non-SMC subunits tagged with the HA epitope were analyzed (Fig. 1 D), proportional amounts of Smc2p and Smc4p were detected for each of the tagged subunits, as determined by densitometry. This result suggests that Brn1p, Ycs4p, and Ycs5p are present in 1:1:1 ratio in the complex. To determine the stoichiometry of the SMC condensin subunits to Brn1p, Ycs4p, and Ycs5p, we performed a small-scale immunoaffinity purification of condensin. One of the non-SMC subunits, Ycs5p, was used to introduce the affinity tag. The protein extract containing Ycs5p-HA was incubated with the anti-HA tag antibodies #2973 (see Materials and Methods) followed by binding to protein A–Sepharose. After elution with the corresponding peptide, composition of the eluate was investigated using PAGE and Western blot (Fig. 1 E). Results of this experiment suggest that all five subunits are present in equimolar ratio, without any additional subunits of comparable molecular mass. Whether any substoichiometric subunits are present in *S. cerevisiae* condensin remains to be determined.

The SMC Components of S. cerevisiae Condensin Are Required for Chromosome Segregation and Condensation

Studies in *X. laevis*, *B. subtilis*, and *S. pombe* predict that Smc2p and Smc4p may be in direct contact with DNA (Kimura and Hirano, 1997; Sutani and Yanagida, 1997; Hirano and Hirano, 1998). We also have shown that at least half of the Smc2p and Smc4p pool is tightly associated with chromatin throughout the cell cycle (see below). Thus, we focused our chromosome segregation and condensation studies on the SMC component of the condensin complex, Smc2p and Smc4p. We used novel conditional alleles of *SMC2* and *SMC4* for detailed functional studies.

The *smc2-8* and *smc4-1* mutants undergo growth arrest within one generation time (Fig. 2 A), accompanied by a decrease in cell viability (Fig. 2 B). At the restrictive temperature, the impairment of chromosome segregation was evident in both the *smc2-8* and *smc4-1* strains, judging by morphology of their nuclear DNA (Fig. 2, C and D). The terminal phenotype of the mutants was consistent with a defect in mitotic chromosome segregation, specifically a defect in full separation of sister chromatids during anaphase. Surprisingly, however, we did not detect an elevated rate of chromosome III loss at 23°C, 35°C after a 3-h shift to 37°C (data not shown).

To investigate the chromosome segregation defect in *smc2-8* and *smc4-1* cells, we used the in vivo chromosomal tag approach (Straight et al., 1996). A plasmid expressing LacI-GFP and an array of *LacO* sites was introduced into the *ura3* locus on chromosome V (see Materials and Methods) in the *smc* mutants and in the isogenic Smc^+ cells. At nonpermissive temperature, both *smc2-8* and *smc4-1* cells showed an increase in the frequency of cells with signals from two sister chromatids located in different cell bodies that are not separated to the maximum possible distance (Fig. 2 E). This finding agrees with the stretched chromosomal DNA morphology frequently seen in these mutants. Thus, the anaphase-like morphology of condensin mutant arrest suggests that the associated block in cell division is determined by improper anaphase progression. Such arrest is analogous to the *top2* phenotype and could be attributed to entanglement of sister chromatids (Spell and Holm, 1994). Thus, the cell division arrest in the *smc2-8* and *smc4-1* mutants could be a result of inability to separate sister chromatids in anaphase completely. Analysis of the same alleles using chromosomal GFP tags did not reveal, however, any defect in the establishing of sister chromatid cohesion (not shown).

Chromosome condensation, if impaired, can cause chromatids to entangle and prevent their proper separation and anaphase completion. In budding yeast, mitotic chromosome condensation has been characterized mainly through FISH using a procedure involving chromatin spreading (Guacci et al., 1994). We attempted to assess chromosome condensation in intact yeast cells using two approaches. In one case, the distance between two *LacO* tags introduced into the *ura3* and *met6* loci was monitored (chromosome V, 225 kb apart). In another strain, the area occupied by the Sir2p-GFP signal (rDNA chromatin) was studied throughout the cell cycle. In both instances, using intact cells and GFP chromosomal tags did not provide sufficient resolution to detect mitotic chromosome condensation (Strunnikov, A., unpublished observation). Thus, FISH remains the only method that allows observation of chromosome condensation in *S. cerevisiae*. Therefore, we used FISH to investigate mitotic changes in chromatin packaging, referred to as condensation.

Previous results suggested that the *SMC2* gene has a role in the maintenance of mitotic chromosome condensa-

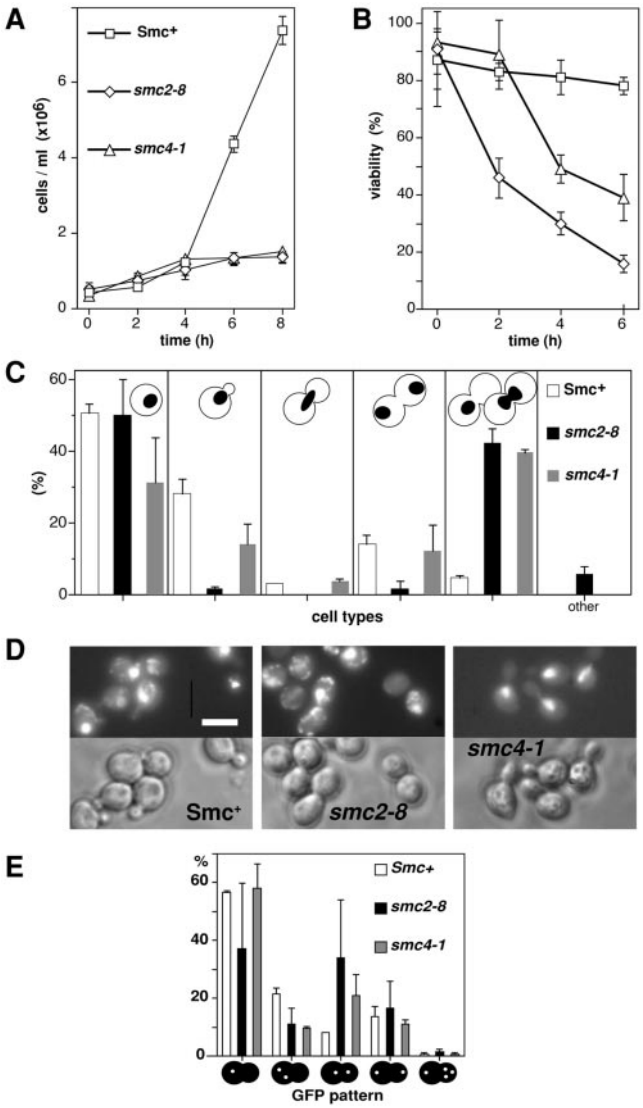

Figure 2. Characterization of *smc2-8* and *smc4-1* mutants. (A) Growth curves of *smc* mutants (strains 1bAS330 and 1bAS344) at 37°C, compared with the isogenic strain YPH499 (Smc^+). (B) Viability of Smc^+ and Smc^- strains (YPH499, 1bAS330, and 1bAS344) at 37°C determined by plating assay. (C) Distribution of cell types within arrested populations of *smc* mutants (strains listed in A) after a 3-h exposure to restrictive temperature (37°C). (D) Cell morphology (phase-contrast) and nuclear DNA position (4,6-diamidino-2-phenylindole staining) in *smc* mutant strains after a 3-h exposure to 37°C. Bar, 5 μm. (E) Sister chromatid separation in wild-type cells and *smc* mutants with a GFP tag at the *ura3* locus after 3 h at 37°C. *Smc*$^+$: YPH499bV; *smc2-8*: 1bAS330bV; *smc4-1*: 1aAS342bV. The classes of cells are as follows (only cells with buds were counted): single dot in any cell body; two dots in the same cell body; one dot in each cell body with the distance between two dots $<2/3$ of maximal cell axis; one dot in each cell body with the distance between two dots $>2/3$ of maximal axial measurement; more than two dots per mother and daughter cell body.

tion (Strunnikov et al., 1995). No assessment of the contribution of Smc2p, Smc4p, or other condensin subunits in the establishment of the condensed state has been made to date. We used FISH to evaluate the input of Smc2p and Smc4p in the establishment of mitotic chromosome condensation. Smc^+, *smc2-8*, or *smc4-1* cells were arrested with α-factor and released from the G1 arrest into nocadazole-containing media at 37°C. This experimental protocol ensures that each strain progresses synchronously through S phase and then arrests at the same point in G2/M while a given temperature-sensitive protein is inactivated (Guacci et al., 1997). Mitotic chromosome condensation was visualized by FISH using an rDNA probe (Fig. 3, A and B) or a series of chromosome VIII arm probes (chromosome painting) (Fig. 3, C and D). We used a novel approach to quantify changes in mitotic chromosome condensation in *S. cerevisiae*. Previously, no quantification has been published for rDNA locus condensation, and the published estimates for nonrepetitive region condensation were based on linear measurements, incompatible with the multiprobe approach. In contrast, we applied area measurements of FISH signal corresponding to a chromosomal domain (Fig. 3). Fig. 3, B and D show that the *smc2-8* and *smc4-1* mutations result in reduced mitotic chromosome condensation at the rDNA locus and in the chromosome VIII arm compared with the Smc^+ cells.

Thus, the *smc2-8* and *smc4-1* mutants have a defect in chromosome transmission and mitotic chromosome condensation. Phenotypic analysis of the *smc2-8* and *smc4-1* mutants did not, however, explain why these mutants display no increase in chromosome loss either at semipermissive or at restrictive (transient shift) conditions, especially taking into account the abnormal mitotic chromosome structure and evident signs of mitotic block. We investigated this phenomenon in a series of experiments designed to evaluate the consequences of condensin impairment on different chromosomes and distinct chromosomal domains.

The SMC2 and SMC4 Genes Have a Specific Role in rDNA Chromatin

Despite the fact that the *smc2-8* and *smc4-1* mutants affect condensation of both unique and repetitive regions of the genome, the different chromosomal domains could have specific requirements for mitotic compaction and thus might be differentially affected by condensation failure and subsequent anaphase block. In this case, some chromosomes may be more sensitive to the loss of condensin function than others. To test whether there is a bias in condensin binding to different chromatin domains, we investigated localization of condensin complex in live intact cells. Previous localization data were obtained using fixed cells overexpressing Smc2p-HA (Strunnikov et al., 1995). Under these conditions, a uniform nuclear signal was observed independently of the cell cycle stage. Using intact live cells and a more sensitive detection system in the absence of protein overexpression allowed us to reveal some novel features of condensin localization in vivo. We followed localization of condensin in intact yeast cells using Smc4p-GFP as a marker. The choice of Smc4p was due to the observation that its intracellular amount does not change in the course of the cell cycle. In an asynchronous cell population expressing Smc4p-GFP from the *SMC4* promoter, the GFP signal was seen either as a diffuse nuclear signal or as concentrated in a subnuclear compart-

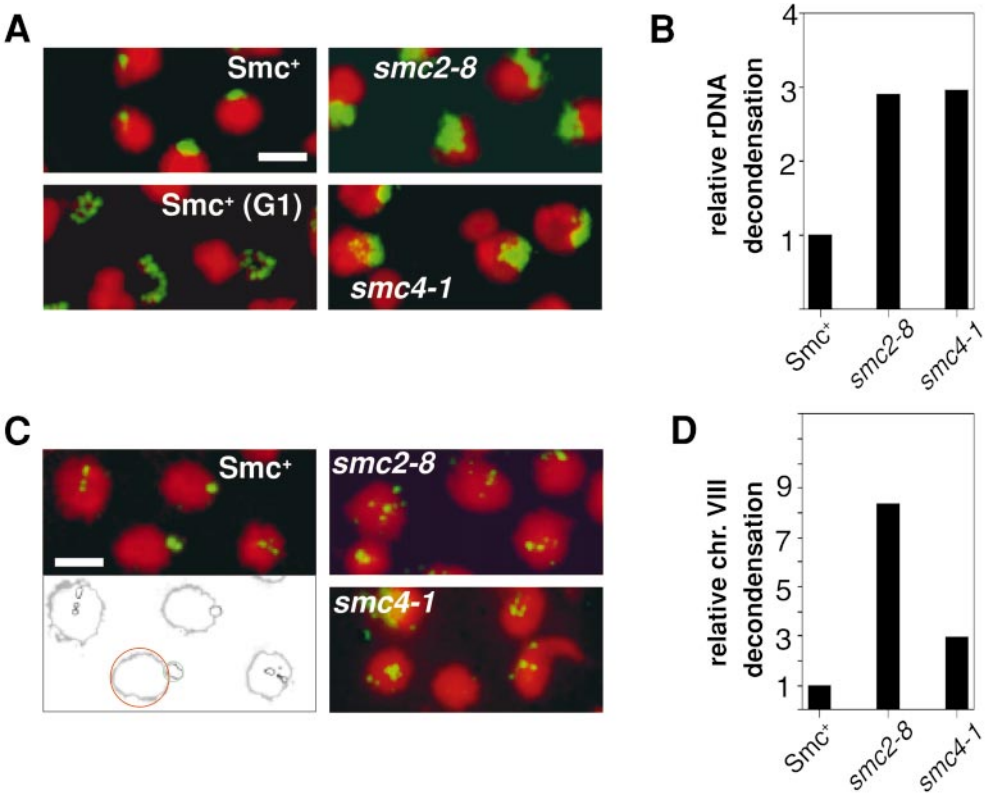

Figure 3. Establishment of rDNA condensation is impaired in *smc* mutants. (A) rDNA FISH. Red, propidium iodide staining corresponding to nuclear DNA; green, rDNA FISH signal. α-Factor–arrested Smc$^+$ cells are shown for comparison. *Smc*$^+$: YPH499b; *smc2-8*: 1bAS330b; *smc4-1*: 1aAS-342b. Bar, 5 μm. (B) Quantitative analysis of condensation of the rDNA locus normalized to the Smc$^+$ value. Arrest conditions, quantification approach, and correction to minimize contribution of cell-to-cell differences in spreading are described in Materials and Methods. (C) Chromosome VIII multiprobe FISH painting. Strains are as in A. A minimal circle was used as an approximation of the area occupied by fluorescent signals (see Materials and Methods). Bar, 5 μm. (D) Quantitative analysis of condensation of chromosome VIII normalized to the Smc$^+$ value.

ment at the nuclear periphery (Fig. 4 A). The shape and position of this compartment is consistent with it being a part of nucleolus (Yang et al., 1989). We confirmed that the area of intensive staining indeed corresponds to nucleolar chromatin by demonstrating that the nucleolar Smc4p-GFP signal is absent in strain NOY891 lacking rDNA repeats (Oakes et al., 1998) (see Materials and Methods). Only a diffuse nuclear GFP signal was observed in NOY891/pLF640 (Fig. 4 C). In the mitotic cells expressing both GFP-tagged Smc4p and Sir2p-GFP, an established rDNA binding protein (Fritze et al., 1997; Gotta et al., 1997), the GFP signal was detected in a subnuclear region of the same shape and position as in the mitotic cells expressing either of the constructs alone (data not shown). Immunofluorescent staining for Net1p-MYC (Shou et al., 1999), a nucleolar protein, largely colocalized with the Smc4p-GFP signal, although the GFP signal was significantly diminished by fixation even as short as 5 min (Fig. 4 D). Observation of a synchronized cell population (Fig. 4 E) established that the subnuclear concentration of Smc4p-GFP is a cell cycle–dependent event. The diffuse nuclear GFP signal observed in interphase cells becomes concentrated in this subnuclear domain before mitosis and persists throughout chromosome separation. This finding indicates that the condensin complex may have a special role in the structure of rDNA chromatin and possibly in mitotic transmission of chromosome XII harboring the ribosomal DNA locus.

Using the Sir2p-GFP marker we followed the rDNA locus position after a 3-h shift to nonpermissive temperature (Fig. 5 A). Surprisingly, we found that in most cells, rDNA did not segregate or even separate into two sister chromatids. Under the same conditions, the pericentromeric regions of chromosome V and the distal arm region of chromosome IV readily separated in more than half of the large-budded cells (Fig. 5, B and C, respectively). Thus, the mutants in the genes for condensin subunits arrest in the middle of anaphase after the separation of chromatids is triggered, but fail to segregate rDNA. Delayed segregation of rDNA is not observed in wild-type yeast cells (Granot and Snyder, 1991). The delay or block in rDNA segregation thus reflects the specific property of condensin mutants. This suggests that condensin may have a more specific role in segregating the rDNA locus, which is structured as an array of tandem 9-kb repeats. To verify whether the tandem repeat structure of the rDNA array plays an important role in its delayed or stalled segregation, we tested the mitotic stability of a plasmid carrying a single rDNA repeat (Nierras et al., 1997). Mitotic stability of the plasmid (81 ± 1% for the Smc$^+$ strain) was only moderately affected by the presence of the *smc2-8* (70 ± 1%) or *smc4-1* (76 ± 1%) mutations.

Does delayed segregation of rDNA in the *smc2-8* and *smc4-1* mutants result in the subsequent loss of this chromosome? Unfortunately, any direct assessment of chromosome XII loss in budding yeast is not feasible, as chromosome XII aneuploidy is probably a lethal event (Granot and Snyder, 1991). To circumvent this limitation,

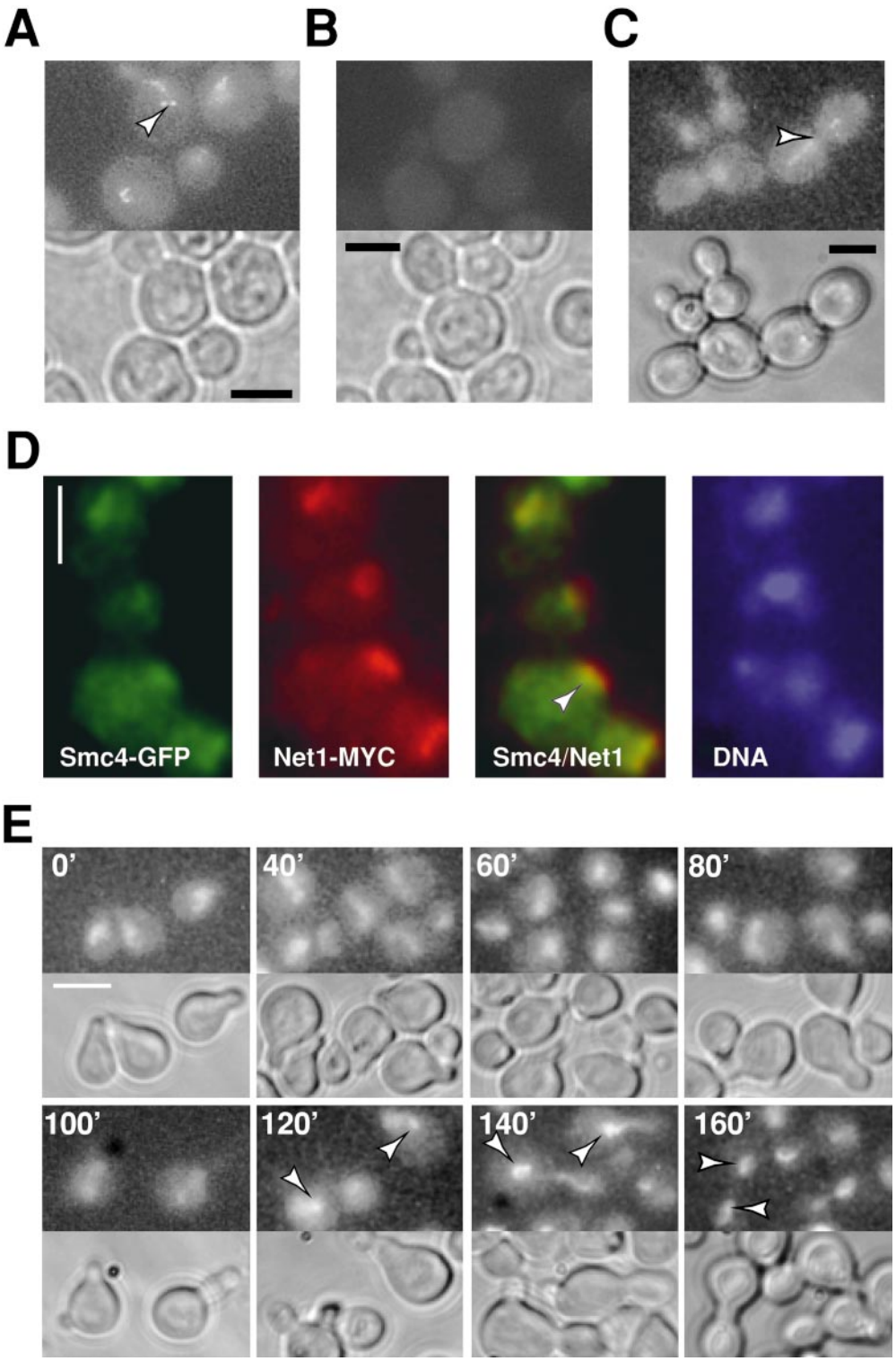

Figure 4. Condensin localization. (A) Condensin localization visualized by Smc4p-GFP in AS335/pLF640 diploid strain grown asynchronously. Arrowhead points to two nucleolar chromatin signals in one nucleus. (B) AS335 without pLF640: negative control for autofluorescence. (C) Strain NOY891/pLF640 lacking rDNA tandem repeats: subnuclear clustering of Smc4p-GFP signal is replaced by diffuse nuclear signal. Arrowhead points to diffuse GFP signal along the putative position of the spindle. (D) Colocalization of Net1p and condensin. Strain WY53 (Shou et al., 1999) was transformed with pLF640, allowing simultaneous detection of Smc4p-GFP (green) and Net1p-MYC (red, anti-MYC antibody, Cy3-conjugated secondary antibody). Arrowhead in the overlap panel points to the nucleolar region. Cells were released from nocadazole block for 30 min, fixed for 5 min with formaldehyde, and processed for immunofluorescence. DNA was visualized with 4,6-diamidino-2-phenylindole. (E) Time course analysis of YPH499b/pLF640 expressing Smc4p-GFP after release from G1 arrest (α-factor) at 23°C in selective media. GFP and phase-contrast images are shown. Arrowheads indicate subnuclear signal corresponding to nucleolar chromatin. Bars, 5 μm.

we used strains homozygous for the *smc2-8* or *smc4-1* mutation but heterozygous for the rDNA locus translocation (Mikus and Petes, 1982). One homologue of chromosome III, a well-marked small chromosome, carried a translocation of the rDNA locus marked with *ADE2* and *LEU2* (Fig. 5 D). The *MAT* locus at the opposite arm of chromosome III was used to distinguish gene conversion events from chromosome loss. The mitotic stability of the rDNA-carrying chromosome III was assayed in Smc^+, *smc2-8*, and *smc4-1* cells using a modification of the half-sector assay (Koshland and Hieter, 1987; Hegemann et al., 1988) (Fig. 5 E). To estimate the loss rate, the cells were grown at the nonpermissive temperature (37°C) for 6 h and then plated and allowed to form colonies at the permissive temperature (30°C). Loss of the *ADE2* marker with simultaneous loss of *LEU2* and *MATa* markers was considered a

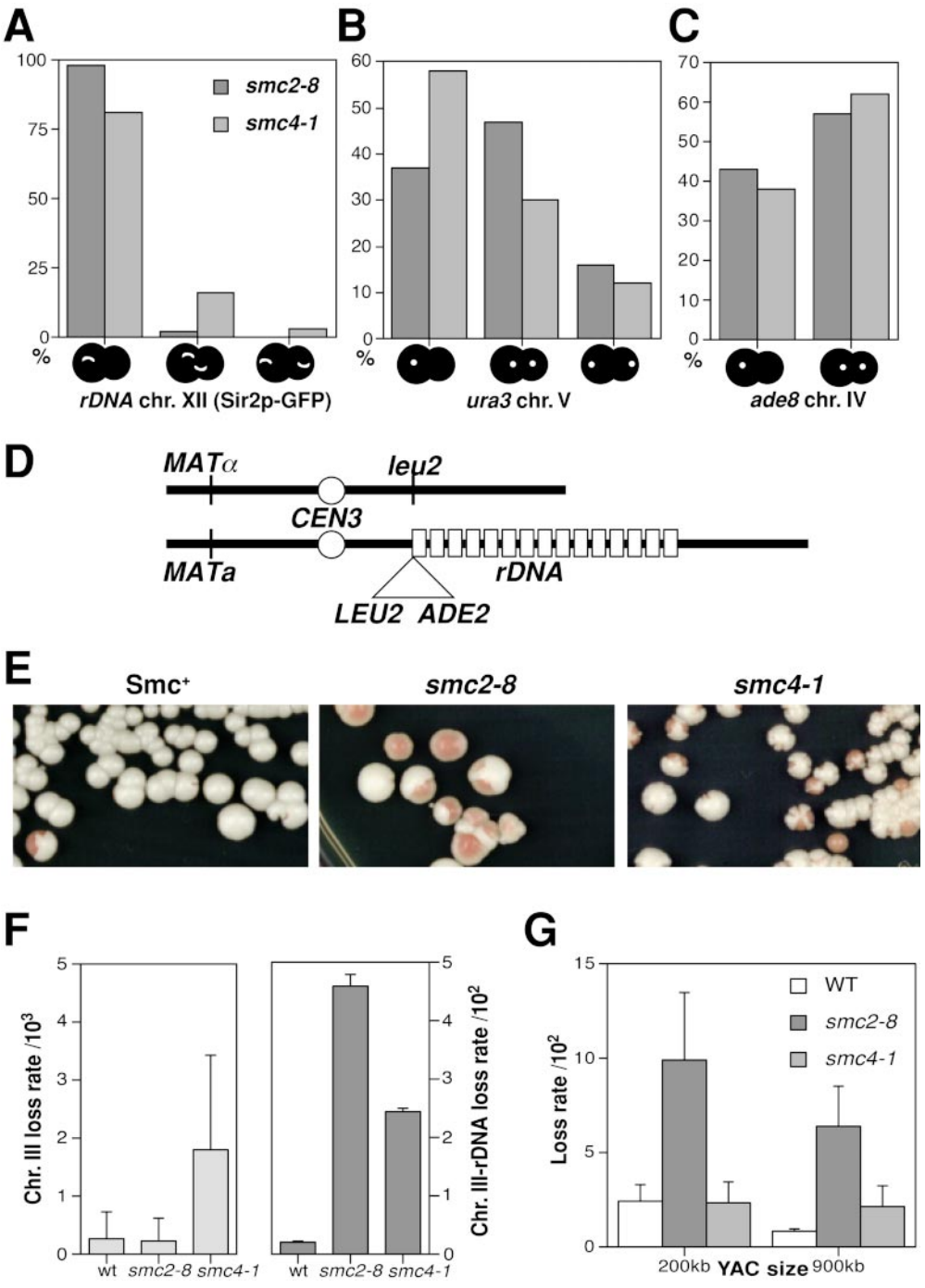

Figure 5. Segregation of the rDNA locus is impaired in condensin mutants. (A) rDNA segregation after a 3-h shift to 37°C in the strains 3-1bAS330b/pAS622 (*smc2-8*) and 6-1bAS344b/pAS622 (*smc4-1*). rDNA was visualized by GFP fused to Sir2p. Only budded cells were scored. Numbers indicate percentage of the given cell type among budded cells. (B) Segregation of pericentromeric *ura3* locus after a 3-h shift to 37°C in the strains 1bAS330bV (*smc2-8*) and 1aAS342bV (*smc4-1*). The chromosomal tag at *ura3* was visualized by GFP fused to LacI. Only budded cells were scored. (C) Segregation of the centromere-distal (850 kb from *CEN4*) *ade8* locus after a 3-h shift to 37°C in the strains 1bAS330bIV (*smc2-8*) and 1aAS342bIV (*smc4-1*). The chromosomal tag at *ade8* was visualized by GFP fused to LacI. Only large-budded cells were scored. (D) Schematic of two chromosome III homologues in strains AS389, AS388, and AS386 used for experiments in E and F. (E) Loss of the rDNA-carrying chromosome III in Smc$^+$, *smc2-8*, and *smc4-1* diploid strain at 35°C. Red sectors correspond to chromosome loss events. The sectoring in Smc$^+$ (diploid strain AS389) is due to *ADE2* loss as a result of mitotic recombination. (F) Comparison of the *ADE2*-marked native chromosome III loss in strains AS260–1 (*wt*), AS359–1 (*smc2-8*), and AS362–1 (*smc4-1*) to the loss of the rDNA-carrying chromosome III in AS389 (*wt*), AS388 (*smc2-8*), and AS386 (*smc4-1*) diploid strains after a transient 6-h shift to 37°C. (G) Loss rates of a 200-kb YAC in strains 4419 (*wt*), 2aAS415 (*smc2-8*), and 1aAS416 (*smc4-1*), compared with the loss rates of a 900-kb YAC in strains 6228 (*wt*), 5bAS413 (*smc2-8*), and 1aAS414 (*smc4-1*) after a 6-h shift to 37°C.

chromosome loss event. Loss of *ADE2* only was considered a mitotic recombination event. In the Smc$^+$ strain, no loss of the rDNA-carrying chromosome III was detected (frequency below 3.4×10^{-5} per cell division). All events of *ADE2* loss shown for the wild-type strain in Fig. 5 E were the result of mitotic recombination (2.1×10^{-3}). In contrast, in the *smc2-8* and *smc4-1* mutants, loss rates were high: 4.6×10^{-2} and 2.4×10^{-2}, respectively. Thus, although *smc2-8* and *smc4-1* only marginally affect transmission of normal chromosome III (Fig. 5 F), these mutants do affect transmission of chromosome III when it is carrying rDNA. This provides genetic evidence that the *SMC2* and *SMC4* genes, and likely the condensin complex as a whole, have a specialized role in the transmission of rDNA in mitosis.

To exclude the possibility that the detected destabilization of chromosome III upon rDNA translocation is due simply to the change in chromosome length, we conducted

an independent test assessing how chromosome length affects its stability in the *smc2-8* and *smc4-1* mutants. Two homologous telocentric yeast artificial chromosomes (YACs) marked with *ADE2* and *HIS3* (Van de Vosse et al., 1997), 200 and 900 kb long, were introduced into the mutant and wild-type strains. The length of the YAC arms roughly corresponds to the arm length of chromosome III without and with rDNA translocation, respectively. The loss rate was measured in the half-sectoring assay after a 6-h shift to 37°C. As expected, the longer YAC generally had higher mitotic stability than the shorter YAC in all strains tested (Fig. 5 G). This result excludes the possibility that chromosome III carrying the rDNA translocation is destabilized in the *smc2-8* and *smc4-1* mutants due to its increased size.

Despite the fact that condensin plays an important role in rDNA structure, the function of condensin is still essential in the absence of the tandemly repeated rDNA genes. When the condensin subunit genes were disrupted in the strain AS401, where the only source of rRNA was a plasmid-borne rDNA repeat (Oakes et al., 1998), the haploid progeny containing disruption alleles of *SMC2*, *SMC4*, *BRN1*, *YCS4*, or *YCS5* could not be recovered. Thus, these genes are still essential for viability in cells without tandem organization of the rRNA genes. Direct integration of the *smc2-8* allele in a strain without the rDNA array resulted in a tight temperature-sensitive phenotype (not shown), suggesting the possibility that in the absence of the array, the secondary sites of condensin binding become more affected.

Condensin Binds to rDNA Chromatin Throughout the Cell Cycle

Is condensin physically present at rDNA or are the observed defects in rDNA condensation and segregation indirect? First, we determined whether condensin binding to bulk chromatin changes throughout the cell cycle using a crude chromatin-binding assay (Liang and Stillman, 1997). Extracts of asynchronous cells or cells arrested in G1, S, or M phase expressing Smc2p-HA were fractionated into a chromatin-bound fraction (pellet) and a chromatin-unbound fraction (supernatant). Hmo1p, a homologue of known chromatin component HMG1 (Lu et al., 1996), associates with chromatin throughout the cell cycle (Fig. 6 A). Smc2p-HA is partially chromatin-bound and partially extractable, and this distribution does not significantly change throughout the cell cycle. Thus, Smc2p may be used to identify the constitutive sites binding condensin in vivo.

For a detailed analysis of Smc2p binding to chromatin throughout the cell cycle, we turned to ChIP analysis of Smc2p-HA binding to the rDNA locus (Fig. 6, B and C). Cells were cross-linked with 1% formaldehyde, chromatin extracts were prepared, and processed for ChIP as described (Meluh and Koshland, 1997). A small aliquot was removed for input sample and the remainder was used for immunoprecipitations with anti-HA antibody. The isogenic strain without a HA tag was used to determine proper template dilution and was included as a negative control in every experiment. After reversing DNA–protein cross-links, immunoprecipitated DNA was purified and analyzed by PCR using a set of primers spanning the rDNA locus (Fig. 6 C). In the asynchronous population, multiple sites of Smc2p-HA binding to rDNA chromatin were detected (Fig. 6 B). To quantify this association, we used synchronized cell populations and compared G1 chromatin to G2/M chromatin (Fig. 6 D), when rDNA is expected to be at its most decondensed and most condensed stages, respectively (Fig. 3 A). Fig. 6 D shows that in α-factor–arrested cells, Smc2p-HA binds to the region upstream of the rDNA replication origin (ARS) (probes 1 and 2) but not to the ARS itself (probe 3). Smc2p binds strongly to the Pol1 promoter (probes 4 and 5) but weakly to the 5′ region of the 37S rDNA transcription unit (probes 6–9), with stronger binding towards the 3′ end of the transcription unit (probes 10–17). Strong binding for α-factor–arrested cells is observed at the replication fork barrier (probe 18) and between the replication fork barrier and the ARS (probes 19–21 and probe 2). The pattern of Smc2p binding to rDNA in nocadazole-arrested cells is very similar to the pattern observed for α-factor–arrested cells, with the notable exception that Smc2p binding 3′ to the replication fork barrier (RFB) and 5′ to the ARS (probes 19–21 and probe 2) and 5′ to the RFB (probe 17) is weaker in nocadazole-arrested cells than in α-factor–arrested cells.

ChIP analysis of the non-SMC condensin subunit Ycs5p revealed even more complexity in the binding of condensin to the rDNA repeat. For Ycs5p-HA association with rDNA, some cell cycle dependence was observed. In G1 cells, only five sites are strongly associated with Ycs5p (probes 10, 11, and 13–15), whereas in G2/M cells a strong correlation with the Smc2p-bound sites is observed. Most notably, the Pol I promoter sites and the 3′ end of the large transcription unit are occupied by Ycs5p in mitosis. Probe 12 again reveals incompatibility of the corresponding region with condensin binding. This result confirms condensin preference for particular binding sites within the rDNA repeat and reveals some heterogeneity between these binding sites. Some of the condensin-binding sites likely have the complete condensin complex bound throughout the cell cycle (probes 13–15), whereas others are associated only with the SMC condensin component in G1 and assemble the full condensin complex only in G2/M. Thus, we presented data pointing to three coexisting modes of condensin recruitment to rDNA. The first mode is constitutive binding of SMC subunits to the specific sites from G1 to mitosis (Smc2p ChIP results), the second is recruitment of additional condensin complexes to rDNA in a mitosis-specific manner (Smc4p-GFP microscopy), and the third, the most speculative, is the mitosis-specific recruitment of the non-SMC subunits to the bound SMC subunits (Ycs5p ChIP data). Repeated structure of rDNA array prevented us from making a quantitative estimate of the relative contributions of these three modes of condensin targeting to rDNA.

Thus, we have identified the first site that is bound by condensin in vivo and uncovered both cell cycle–dependent and cell cycle–independent components in this association. However, condensin binding is not strictly limited to rDNA, as we found several additional sites in the genome, including pericentromeric and peritelomeric regions, that showed association with condensin in the ChIP assay (Freeman, L., unpublished observations), in agree-

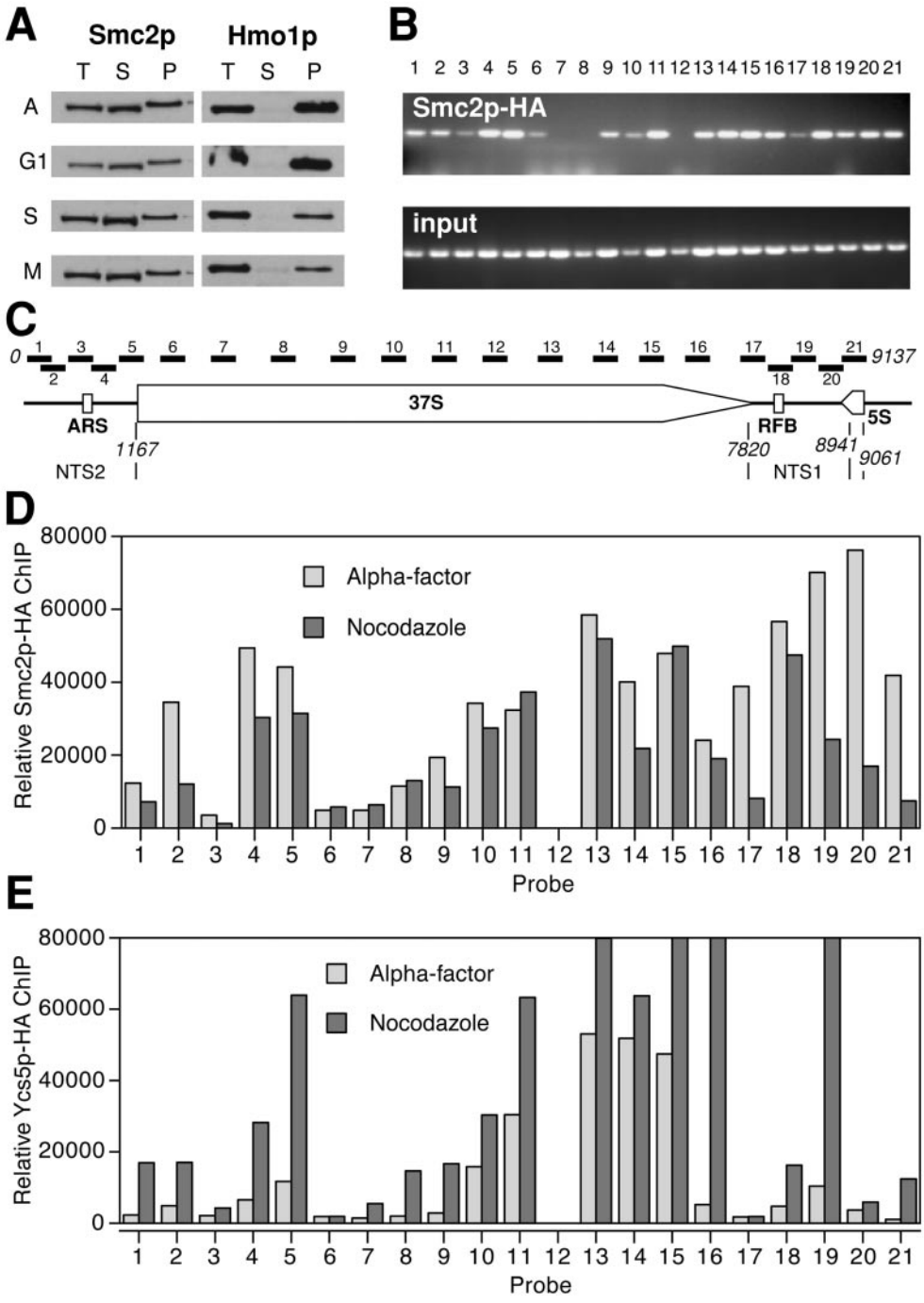

Figure 6. Condensin binding to chromatin at the rDNA locus. (A) A significant portion of Smc2p is chromatin-bound throughout the cell cycle. Chromatin binding of Smc2p and Hmo1p (a reference chromatin protein) throughout the cell cycle determined by chromatin solubilization assay (Liang and Stillman, 1997). Strain YPH499bp2 was grown asynchronously or arrested in G1, S, or G2/M phase. Lysates were centrifuged to yield a chromatin-unbound fraction (supernatant 2 according to Liang and Stillman [1997]) and a chromatin-bound fraction (pellet 3). Unfractionated lysate (T), supernatant (S), and pellet (P) were probed with antibodies to Smc2p and Hmo1p (Lu et al., 1996). (B) Agarose gel electrophoresis of ChIP analysis of the rDNA repeat in the asynchronously growing YPH499bp2 strain with PCR probes shown in C. (D) Quantification of the Smc2p-HA ChIP in strain YPH499bp2 arrested with α-factor and nocadazole. The PCR signals were quantified using ImageQuant (Molecular Dynamics). All volume scans were normalized to the signal from probe 12 that was only marginally above background (Relative ChIP) and to the corresponding PCR on the input DNA. (E) Quantification of the Ycs5p-HA ChIP in strain YPH499bp5 arrested with α-factor and nocadazole. Analysis was as in Fig. 5 D.

ment with FISH data (Fig. 3, C and D). Functional analysis of condensin binding to these sites in strains without the tandem rDNA array is under way.

Discussion

The Condensin Complex of S. cerevisiae

The *S. cerevisiae* genome sequence reveals the presence of five genes encoding proteins homologous to the *X. laevis* condensin subunits (Kimura et al., 1999). We have demonstrated that these five genes encode subunits of the *S. cerevisiae* condensin complex. All five *S. cerevisiae* condensin subunits are essential for cell viability. The core SMC subunits, Smc2p and Smc4p, were tested and found to be essential for chromosome condensation. We have demonstrated that the condensin complex containing all five subunits is present throughout the cell cycle and has a complex mode of interaction with chromatin. Thus, condensin from *S. cerevisiae* bears remarkable similarity to the previously characterized 13S condensin from *X. laevis* and *S. pombe* condensin (Kimura et al., 1999, Sutani et al., 1999).

Despite these similarities, differences between the con-

densin complexes of different species were found when their cell cycle behavior was examined. *S. cerevisiae* condensin localization shows a prominent cell cycle–dependent change at the subnuclear level. Smc4p-GFP exhibits a mostly diffuse nuclear staining pattern during most of the cell cycle but shows nucleolar localization at G2/M. Both Smc2p and Smc4p bind chromatin throughout the cell cycle, as assayed by a crude chromatin-binding assay. Further refinement using ChIP analysis revealed that Smc2p binds specific chromatin sites both in G1 and in G2/M phases. Ycs5p binds to many of these sites only in G2/M. Cell cycle–regulated binding of non-SMC condensin subunits to constitutively bound SMC condensin components thus appears to be a unique feature of the *S. cerevisiae* condensin complex. In contrast, in *S. pombe*, the entire complex translocates to the nucleus at mitosis. This translocation is due to phosphorylation of a specific site in Cut3, an Smc4p homologue (Sutani et al., 1999). In *X. laevis*, phosphorylation of the non-SMC components of condensin is responsible for chromosomal targeting of the condensin complex at mitosis and for the positive supercoiling activity of the condensin (Kimura et al., 1998). In this case, phosphorylation occurs on the non-SMC subunits of the *X. laevis* condensin complex.

The mechanism of regulation of *S. cerevisiae* condensin activity and targeting throughout the cell cycle still remains to be elucidated. We found no evidence of nuclear import being involved in condensin regulation. We also demonstrated that expression levels of SMC proteins in the condensin complex do not vary throughout the cell cycle, whereas transcription (Spellman et al., 1998) and protein levels of *BRN1*, *YCS4*, and *YCS5* are under only mild cell cycle control (data not shown). It is therefore unlikely that expression level is the regulatory mechanism responsible for the cell cycle control of condensin activity in *S. cerevisiae*. Regulation of *S. cerevisiae* condensin activity by posttranslational modifications is an open possibility, although neither of the phosphorylation sites identified in *X. laevis* or *S. pombe* condensin are conserved in *S. cerevisiae* condensin.

In conjunction with the observations discussed above, it is clear that onset of mitosis induces a fundamental and complex change in the nature of chromatin-bound condensin complex. This study is focused on the biological role of chromatin condensation in budding yeast and on characterization of the functionally critical chromatin sites affected by condensin activity.

Condensin and Mitotic Chromosome Transmission

Previous observation of bulk nuclear DNA in the *smc2-6* mutant has established that chromosome transmission in mitosis is disrupted in this mutant. Here we demonstrate that both the novel temperature-sensitive allele *smc2-8* as well as the *smc4-1* mutation in the newly characterized *SMC4* gene impair proper partitioning of chromosomes in mitosis (Fig. 2 E). Both of these mutants also disrupt establishment of mitotic condensation of rDNA and chromosome VIII (Fig. 3), suggesting that this defect may be responsible for the resulting chromosome segregation block. This reinforces previous conclusions that one biological role of condensin in vivo is to establish the higher order structure of mitotic chromosomes necessary for successful sister chromatid separation at anaphase (Koshland and Strunnikov, 1996).

Since the initial characterization of the *smc2* mutant, one question has, however, remained unresolved: why obvious impairment of mitosis in a condensin component mutant does not translate into a genetically tractable event of chromosome loss and/or nondisjunction. We find that mutations in condensin components can indeed be detected genetically as chromosome instability, but the effect depends on the composition of the chromosome. The presence or absence of rDNA on a chromosome affects its loss rate in condensin mutants.

S. cerevisiae chromosomes lacking rDNA appear to show only a transient block in mitotic segregation in condensin mutants. A typical *S. cerevisiae* chromosome contains mostly unique nonrepetitive DNA, with the exception of the telomeric regions. For such chromosomes, exemplified by chromosomes III, V, and IV analyzed here, a high frequency of separated, properly oriented chromatids that did not complete anaphase B (Fig. 2 E and Fig. 5 B) is observed in condensin subunit mutants. There is also evidence that chromosomal arms frequently exhibit delayed segregation (Fig. 5 C). Yet increased loss of chromosome III is not observed in these mutants. It is not presently known whether this anaphase lock is due to an unknown feedback control arresting the cell cycle at anaphase or to the structural interlocks between the chromatid arms holding them together. The genetic interaction of condensin subunit mutants with topoisomerase mutants (Saka et al., 1994; Bhat et al., 1996) and the supercoiling activity of condensin in vitro (Kimura et al., 1999) support the latter theory. We can hypothesize that inability to detect high rates of chromosome III loss in our study was due to the eventual resolution of these tangles by topoisomerase II activity, allowing for recovery after the temperature shift and resulting in relatively high viability, despite the clear condensation defects throughout the genome (Fig. 3).

For the rDNA-containing chromosome XII, however, the condensin mutations lead to a phenotype consistent with a virtually complete block of mitotic segregation. In this case, we found an almost complete absence of sister chromatid separation (Fig. 5 A). Unsegregated rDNA resided in one of the cells in the dividing pair, potentially leading to lethality of one half of the newly generated cells. Indeed, both *smc2* and *smc4* mutants display 30–50% viability after the 4-h temperature shift (Fig. 2 B). If nondisjunction had affected other chromosomes, this value should have been significantly lower. These observations, coupled with the impairment of rDNA condensation in condensin mutants, suggest that condensin defects may affect rDNA segregation in a distinct manner.

This hypothesis is supported by our finding that genetic instability of a chimeric chromosome III containing a rDNA translocation increases dramatically in the *smc2* and *smc4* mutants compared with the wild-type cells. More corroborating evidence for this theory is the discovery that condensin localization in vivo is strongly biased towards rDNA. We found that the rDNA array has a high density of Smc2p and Ycs5p binding sites and that Smc4p-GFP

concentrates in the nucleolar region at the G2/M transition. We can speculate that both the high density of binding and the mitotic-specific relocalization reflect the important role of condensin in the formation of higher order structure of the rDNA region. Impaired condensation of the whole rDNA chromosomal region may explain the severity of the defects observed in chromosomes carrying rDNA in the condensin subunit mutants.

Specificity of Condensin Binding to Chromatin

The data presented in this study argue that in a cell containing a chromosomal rDNA array, an essential function of condensin is to properly condense and thus facilitate segregation of this chromatin domain. ChIP analysis of condensin binding to rDNA chromatin at 300-bp resolution reported here suggests that condensin binding is strongly biased towards specific chromatin sites. This is the first evidence of such bias in vivo. In vitro, however, condensin preferably binds to structured DNA (Kimura and Hirano, 1997). Thus, we are now in a position to uncover what the rules are for condensin binding to chromatin in live cells. Many factors may contribute to this specificity, such as structure of the underlying DNA, kinetics of chromatin assembly on this DNA, or occupancy of the condensin-specific sites by nonhistone proteins. For example, the rDNA ARS may not be compatible with strong condensin binding due to occupation by the origin recognition complex. At the same time, some condensin binding sites found within the rDNA locus correlate well with known Sir2p and Net1p binding sites in rDNA (Gotta et al., 1997; Straight et al., 1999). A region of condensin binding in the nontranscribed spacer (probes 18–21 in Fig. 6) also correlates well with the major rDNA sir-responsive region SRR1 observed by Fritze et al. (1997), whereas the second described sir-responsive region SRR2 does not appear to correlate with sites of condensin binding. Thus, it appears theoretically possible to identify chromatin proteins, including histones, and corresponding mutants that will interfere with condensin binding or will be indifferent. Mutations in *SIR2* and *NET1*, for example, do not affect condensin targeting (our unpublished observation).

The high density of short inverted repeats in the rRNA genes may itself attract condensin binding, since it has been shown that condensin binding in vitro prefers structured or cruciform DNA (Kimura and Hirano, 1997). This hypothesis correlates well with our experimental result that artificial chromosomes, containing multiple mammalian satellite sequences, were less stable in the *smc2* mutant than in wild-type cells (Fig. 5 G).

It is not known whether the mechanism of condensin activity in rDNA is different from condensin function on other chromosomes. It remains to be determined, probably through a genome-wide approach, what the requirements are for condensin binding to the non-rDNA sites. These sites include the primary sites of condensin binding in the centromeric and subtelomeric regions and the probable secondary sites that are occupied only when the rDNA array is not present. Taken together these data may allow identification of additional essential targets of condensin activity in chromatin.

Condensin Function and the Cell Cycle

When rDNA segregation and centromere-driven segregation are uncoupled, as in strains with the plasmid-borne rDNA, condensin function still remains essential. The provocative findings that the condensin complex is partially assembled on rDNA chromatin throughout the cell cycle opens the possibility that the condensin complex in *S. cerevisiae* may have another role in rDNA chromatin that is not directly associated with mitotic chromosome segregation. Such function may be related to the unique heterochromatin-like properties of the rDNA locus (Bryk et al., 1997, Fritze et al., 1997). Alternatively, binding to the condensation site throughout the cell cycle may provide an effective way to complete condensation in the small window of time allowed by the short yeast cell cycle.

The failure to segregate rDNA in mitosis described here for condensin subunit mutants is reminiscent of the mutant *cdc14* phenotype (Granot and Snyder, 1991). In this mutant the nucleolus fails to segregate, unlike in another late mitotic mutant, *cdc15*. Interestingly, the *cdc14* mutant was found to be defective in rDNA condensation (Guacci et al., 1994), whereas the *cdc15* mutant was not. Cdc14p is an abundant nucleolar protein playing a key role in mitotic regulation (Visintin et al., 1998, 1999; Shou et al., 1999). As condensin is highly enriched in the nucleolus, it is intriguing to speculate that condensin targeting to rDNA chromatin and its function there could be linked to the anaphase entry and exit from mitosis, processes dependent on nucleolar proteins.

We thank G. Fink, A. Straight, A. Murray, E. Jones, S. Brill, S. Liebman, Y. Chernoff, S. Roeder, M. VanDerBerg, J. Den Dunnen, M. Nomura, O. Cohen-Fix, and V. Larionov for research materials; D. Koshland, I. Ouspenski, O. Cabello, V. Zakian, and M. Christman for advice and communicating results before publication; A. Wolffe for the comments on the manuscript; and R. Jenkins for technical help.

L. Freeman and L. Aragon-Alcaide were recipients of the National Institute of Child Health and Human Development Intramural Research Training Awards.

Submitted: 18 May 1999
Revised: 22 March 2000
Accepted: 29 March 2000

References

Bhat, M.A., A.V. Philp, D.M. Glover, and H.J. Bellen. 1996. Chromatid segregation at anaphase requires the barren product, a novel chromosome-associated protein that interacts with Topoisomerase II. *Cell.* 87:1103–1114.

Britton, R.A., D.C. Lin, and A.D. Grossman. 1998. Characterization of a prokaryotic SMC protein involved in chromosome partitioning. *Genes Dev.* 12:1254–1259.

Bryk, M., M. Banerjee, M. Murphy, K.E. Knudsen, D.J. Garfinkel, and M.J. Curcio. 1997. Transcriptional silencing of Ty1 elements in the RDN1 locus of yeast. *Genes Dev.* 11:255–269.

Chuang, P., D. Albertson, and B. Meyer. 1994. DPY-27: a chromosome condensation protein homolog that regulates *C. elegans* dosage compensation through association with the X chromosome. *Cell.* 79:459–474.

Chuang, P.T., J.D. Lieb, and B.J. Meyer. 1996. Sex-specific assembly of a dosage compensation complex on the nematode X chromosome. *Science.* 274: 1736–1739.

Cubizolles, F., V. Legagneux, R. Le Guellec, I. Chartrain, R. Uzbekov, C. Ford, and K. Le Guellec. 1998. pEg7, a new xenopus protein required for mitotic chromosome condensation in egg extracts. *J. Cell Biol.* 143:1437–1446.

Fritze, C.E., K. Verschueren, R. Strich, and R. Easton Esposito. 1997. Direct evidence for SIR2 modulation of chromatin structure in yeast rDNA. *EMBO (Eur. Mol. Biol. Organ.) J.* 16:6495–6509.

Galibert, F., D. Alexandraki, A. Baur, E. Boles, N. Chalwatzis, J.C. Chuat, F. Coster, C. Czieplucha, M. De Haan, H. Domdey, et al. 1996. Complete nucleotide sequence of *Saccharomyces cerevisiae* chromosome X. *EMBO (Eur. Mol. Biol. Organ.) J.* 15:2031–2049.

Gietz, R.D., and A. Sugino. 1988. New yeast - *Escherichia coli* shuttle vectors constructed with in vitro mutagenized yeast genes lacking six-base pair restriction sites. *Gene.* 74:527–534.

Gotta, M., S. Strahl-Bolsinger, H. Renauld, T. Laroche, B.K. Kennedy, M. Grunstein, and S.M. Gasser. 1997. Localization of Sir2p: the nucleolus as a compartment for silent information regulators. *EMBO (Eur. Mol. Biol. Organ.) J.* 16:3243–3255.

Granot, D., and M. Snyder. 1991. Segregation of the nucleolus during mitosis in budding and fission yeast. *Cell Motil. Cytoskelet.* 20:47–54.

Graumann, P.L., R. Losick, and A.V. Strunnikov. 1998. Subcellular localization of *Bacillus subtilis* SMC, a protein involved in chromosome condensation and segregation. *J. Bacteriol.* 180:5749–5755.

Guacci, V., E. Hogan, and D. Koshland. 1994. Chromosome condensation and sister chromatid pairing in budding yeast. *J. Cell Biol.* 125:517–530.

Guacci, V., D. Koshland, and A. Strunnikov. 1997. A direct link between sister chromatid cohesion and chromosome condensation revealed through the analysis of MCD1 in *S. cerevisiae. Cell.* 91:47–57.

Hegemann, J.H., J.H. Shero, G. Cottarel, P. Philippsen, and P. Hieter. 1988. Mutational analysis of the centromere DNA from chromosome VI of *Saccharomyces cerevisiae. Mol. Cell. Biol.* 8:2523–2528.

Hirano, M., and T. Hirano. 1998. ATP-dependent aggregation of single-stranded DNA by a bacterial SMC homodimer. *EMBO (Eur. Mol. Biol. Organ.) J.* 17:7139–7148.

Hirano, T. 1999. SMC-mediated chromosome mechanics: a conserved scheme from bacteria to vertebrates? *Genes Dev.* 13:11–19.

Hirano, T., and T. Mitchison. 1994. A heterodimeric coiled-coil protein required for mitotic chromosome condensation in vitro. *Cell.* 79:449–458.

Hirano, T., R. Kobayashi, and M. Hirano. 1997. Condensins, chromosome condensation protein complexes containing XCAP-C, XCAP-E and a *Xenopus* homolog of the *Drosophila* Barren protein. *Cell.* 89:511–521.

Johnston, M., L. Hillier, L. Riles, K. Albermann, B. Andre, W. Ansorge, V. Benes, M. Bruckner, H. Delius, E. Dubois, et al. 1997. The nucleotide sequence of *Saccharomyces cerevisiae* chromosome XII. *Nature.* 387:87–90.

Kimura, K., and T. Hirano. 1997. ATP-dependent positive supercoiling of DNA by 13S condensin: a biochemical implication for chromosome condensation. *Cell.* 90:625–634.

Kimura, K., M. Hirano, R. Kobayashi, and T. Hirano. 1998. Phosphorylation and activation of 13S condensin by Cdc2 in vitro. *Science.* 282:487–490.

Kimura, K., V.V. Rybenkov, N.J. Crisona, T. Hirano, and N.R. Cozzarelli. 1999. 13S condensin actively reconfigures DNA by introducing global positive writhe: implications for chromosome condensation. *Cell.* 98:239–248.

Koshland, D., and P. Hieter. 1987. Visual assay for chromosome ploidy. *In* Methods in Enzymology. Vol. 155. R. Wu, editor. Academic Press, San Diego, CA. 351–372.

Koshland, D., and A. Strunnikov. 1996. Mitotic chromosome condensation. *Annu. Rev. Cell Dev. Biol.* 12:305–333.

Liang, C., and B. Stillman. 1997. Persistent initiation of DNA replication and chromatin-bound MCM proteins during the cell cycle in cdc6 mutants. *Genes Dev.* 11:3375–3386.

Lieb, J.D., M.R. Albrecht, P.T. Chuang, and B.J. Meyer. 1998. MIX-1: an essential component of the *C. elegans* mitotic machinery executes X chromosome dosage compensation. *Cell.* 92:265–277.

Lu, J., R. Kobayashi, and S.J. Brill. 1996. Characterization of a high mobility group 1/2 homolog in yeast. *J. Biol Chem.* 271:33678–33685.

Meluh, P.B., and D. Koshland. 1997. Budding yeast centromere composition and assembly as revealed by in vivo cross-linking. *Genes Dev.* 11:3401–3412.

Michaelis, C., R. Ciosk, and K. Nasmyth. 1997. Cohesins: chromosomal proteins that prevent premature separation of sister chromatids. *Cell.* 91:35–45.

Mikus, M.D., and T.D. Petes. 1982. Recombination between genes located on nonhomologous chromosomes in *Saccharomyces cerevisiae. Genetics.* 101: 369–404.

Nierras, C.R., S.W. Liebman, and J.R. Warner. 1997. Does *Saccharomyces* need an organized nucleolus? *Chromosoma.* 105:444–451.

Oakes, M., J.P. Aris, J.S. Brockenbrough, H. Wai, L. Vu, and M. Nomura. 1998. Mutational analysis of the structure and localization of the nucleolus in the yeast *Saccharomyces cerevisiae. J. Cell Biol.* 143:23–34.

Rose, M.D., F. Winston, and P. Hieter. 1990. Methods in Yeast Genetics, a Laboratory Course Manual. Cold Spring Harbor Press, Cold Spring Harbor, NY. 234 pp.

Saitoh, N., I.G. Goldberg, E.R. Wood, and W.C. Earnshaw. 1994. ScII: an abundant chromosome scaffold protein is a member of a family of putative ATPases with an unusual predicted tertiary structure. *J. Cell Biol.* 127:303–318.

Saka, Y., T. Sutani, Y. Yamashita, S. Saitoh, M. Takeuchi, Y. Nakaseko, and M. Yanagida. 1994. Fission yeast cut3 and cut14, members of the ubiquitous protein family, are required for chromosome condensation and segregation in mitosis. *EMBO (Eur. Mol. Biol. Organ.) J.* 13:4938–4952.

Shou, W., J.H. Seol, A. Shevchenko, C. Baskerville, D. Moazed, Z.W. Chen, J. Jang, H. Charbonneau, and R.J. Deshaies. 1999. Exit from mitosis is triggered by Tem1-dependent release of the protein phosphatase Cdc14 from nucleolar RENT complex. *Cell.* 97:233–244.

Spell, R.M., and C. Holm. 1994. Nature and distribution of chromosomal intertwinings in *Saccharomyces cerevisiae. Mol. Cell. Biol.* 14:1465–1476.

Spellman, P.T., G. Sherlock, M.Q. Zhang, V.R. Iyer, K. Anders, M.B. Eisen, P.O. Brown, D. Botstein, and B. Futcher. 1998. Comprehensive identification of cell cycle-regulated genes of the yeast *Saccharomyces cerevisiae* by microarray hybridization. *Mol. Biol. Cell.* 9:3273–3297.

Straight, A.F., A.S. Belmont, C.C. Robinett, and A.W. Murray. 1996. GFP tagging of budding yeast chromosomes reveals that protein-protein interactions can mediate sister chromatid cohesion. *Curr. Biol.* 6:1599–1608.

Straight, A.F., W. Shou, G.J. Dowd, C.W. Turck, R.J. Deshaies, A.D. Johnson, and D. Moazed. 1999. Net1, a Sir2-associated nucleolar protein required for rDNA silencing and nucleolar integrity. *Cell.* 97:245–256.

Strunnikov, A.V. 1998. SMC proteins and chromosome structure. *Trends Cell Biol.* 8:454–459.

Strunnikov, A.V., V.L. Larionov, and D. Koshland. 1993. *SMC1*: an essential yeast gene encoding a putative head-rod-tail protein is required for nuclear division and defines a new ubiquitous protein family. *J. Cell Biol.* 123:1635–1648.

Strunnikov, A.V., E. Hogan, and D. Koshland. 1995. *SMC2*, a *Saccharomyces cerevisiae* gene essential for chromosome segregation and condensation defines a subgroup within the SMC-family. *Genes Dev.* 9:587–599.

Sutani, T., and M. Yanagida. 1997. DNA renaturation activity of the SMC complex implicated in chromosome condensation. *Nature.* 388:798–801.

Sutani, T., T. Yuasa, T. Tomonaga, N. Dohmae, K. Takio, and M. Yanagida. 1999. Fission yeast condensin complex: essential roles of non-SMC subunits for condensation and Cdc2 phosphorylation of Cut3/SMC4. *Genes Dev.* 13: 2271–2283.

Van de Vosse, E., P. Van der Bent, J.J. Heus, G.J. Van Ommen, and J.T. Den Dunnen. 1997. High-resolution mapping by YAC fragmentation of a 2.5-Mb Xp22 region containing the human RS, KFSD and CLS disease genes. *Mamm. Genome.* 8:497–501.

Visintin, R., K. Craig, E.S. Hwang, S. Prinz, M. Tyers, and A. Amon. 1998. The phosphatase Cdc14 triggers mitotic exit by reversal of Cdk-dependent phosphorylation. *Mol. Cell.* 2:709–718.

Visintin, R., E.S. Hwang, and A. Amon. 1999. Cfi1 prevents premature exit from mitosis by anchoring Cdc14 phosphatase in the nucleolus. *Nature.* 398: 818–823.

Yang, C.H., E.J. Lambie, J. Hardin, J. Craft, and M. Snyder. 1989. Higher order structure is present in the yeast nucleus: autoantibody probes demonstrate that the nucleolus lies opposite the spindle pole body. *Chromosoma.* 98:123–128.